




Cite this: *RSC Adv.*, 2021, 11, 29711

Imidazolium based ionic liquid stabilized foams for conformance control: bulk and porous scale investigation†

Sivabalan Sakthivel * and Rahul Babu Salin 

Foams are typically used as a divergent fluid for conformance control in order to divert the fluid flow from a high-permeable zone into a low-permeable zone. Nevertheless, the stability of the foam still remains a challenge due to the presence of antifoaming crude oil and the harsh environment of the reservoir, such as high-temperature, high-salinity, and high-pressure. In this study, we investigated the stability and efficacy of various surfactant generated foams with ionic liquid (IL) additives. Intrinsically, the study is targeted to represent the conditions of Arab-D reservoir formations, which are abundant in Saudi Arabian oilfields. In this, we have screened several parameters that influence foam stability like the type of foamer gases (CO₂, N₂, and air), type of ILs, type of surfactants (nonionic, anionic, cationic, and zwitterionic), concentration, salinity (formation brine, low salinity brine, and seawater brine), temperature, etc. The stability of the generated foams was analyzed in both bulk and porous scale media. The bulk foam study has demonstrated that only a very minor concentration of ILs (50–500 ppm) shows a greater improvement in both the foamability and foam stability. The stability of the foam in the presence of the studied ILs and surfactants increases by more than 50% compared to their neat surfactant solution. A similar response was also witnessed in the dynamic foaming experiments at high-temperature, high-pressure, and high-salinity. The current work also involves the determination of the foam morphology, including structure, size, shape, gas–water interface and the lamellae size for different systems with and without ILs, which helps to understand the stability mechanism of the foams with and without ILs. Confocal and optical microscopic images of the foam structure of various systems reveal that these ILs are successful in reducing the size of bubbles and increasing the lamellae size. It is very clear that the addition of ILs generates the surfactant layered-ILs, and they tend to arrange themselves in the lamellae, and at the liquid–gas interface, thereby decreasing the rate of film drainage at the lamellae and delaying the bubble rupture point. This led to the observed enhanced foam stability. Thus, we would like to conclude that the ILs investigated here improved the foam stability by their adsorption at the foam lamella which further helped in preventing liquid drainage and film thinning.

Received 27th June 2021
Accepted 31st August 2021

DOI: 10.1039/d1ra04966f

rsc.li/rsc-advances

1. Introduction

About two-thirds of the world's reservoirs holds a sizable amount of oil that is left unrecovered even after employing primary and secondary oil recovery operations, it is typically called trapped or residual or bypassed oil. It is usually held as an immovable oil, even after the waterflood due to the unfavorable physicochemical properties of the reservoir.¹ In order to tackle these issues, tertiary or enhanced oil recovery (EOR) has been designed to improve oil production. In this, the injection of foreign fluids is employed in the depleted reservoir in order to

alter the physicochemical properties of the reservoir condition and to enable mobilization of trapped or residual oil towards the production well. Various types of EOR methods are implemented in the industry, such as thermal flooding, chemical flooding, gas flooding, microbial methods, etc. Among this, gas flooding is one of the most successful and studied methods for the depleted reservoirs, which contributes to about 39% of recovery among all the EOR methods.^{2,3} Wherein, gases like CO₂, N₂, hydrocarbon and/or the combination of any of these gases are employed at the end of the waterflooding.

However, the early breakthrough with poor sweep efficiency is the most common challenge that is encountered in typical gas flooding. This occurs due to the low density and high mobility of the injection gases than any other resident fluids in the reservoirs, which further leads to gravity override and viscous fingering at the high permeable zone (channeling).⁴ In order to overcome these challenges, the establishment of foamed gas

Center for Integrative Petroleum Research (CIPR), College of Petroleum Engineering & Geosciences, King Fahd University of Petroleum and Minerals, Dhahran-31261, Saudi Arabia. E-mail: sivabalan.sakthivel@kfupm.edu.sa; Tel: +966 (13) 860 3917

† Electronic supplementary information (ESI) available. See DOI: 10.1039/d1ra04966f



injection was developed. In this, the mobility of the dispersed gases in surfactant solution will be retarded by the thin liquid film in the foam, *i.e.*, the lamellae of the surfactant liquid solution.^{5,6} The apparent viscosity of the foam is increased substantially than the neat gases, which causes the reduction of relative permeability for the foams compared to the neat gases. By this method the foams act as a diverging agent to alter the flow direction of the foam from the typical high permeable zone into the unattended low permeable zones.^{7,8} Despite the foam being impressive to control the gas flow, the stability of the foams still remains a challenge at the extreme reservoir conditions, such as high-temperature, high-salinity, and high-pressure.^{9,10} In these harsh environments, the interfacial liquid films (lamellae) of the foams were found to be thinning out so rapidly by the film drainage due to the gravity segregation and high capillary pressure. Subsequently, the inter-bubble gas diffusion and coalescence or bubble rupture would take place to de-stabilize the foams.¹¹ In addition to this, the stability of the foam in the presence of crude oil is another challenge.^{12,13} The effective foam is expected to show better stability even in the presence of oil. Whereas, most studies were demonstrated that the presence of crude oil affects foam longevity to a large extent. Many researchers were proved it by both bulk and porous studies.^{12–17} The foam mobility in the porous media is relatively much faster in the presence of oil than in the absence of oil. It occurs due to the severe detrimental (coarsening) effect of oil, which obviously retards the foam propagation into the deep reservoir.¹² However, which is also depends on several other physico-chemical parameters, such as, pH, oil composition, oil wettability, oil-brine ratio, *etc.*^{12,14,15} Hence, it is very crucial to study the oil-tolerant and stable pseudoemulsion film comprising foams.

The conventional chemicals fail to stabilize the foam in the harsh environment. These chemical additives get degraded or lose their efficiency at the high-temperature and high-salinity, thus it fails to adsorb at the liquid–gas interface, and that leads for the rapid film drainage.^{9,10} Hence, there has arisen a need for a better surface-active agent that helps to strengthen the lamellae film to achieve greater stability, particularly at high salinity, pressure and temperature.^{5,10,18}

Despite several types of chemical additives (electrolytes, nanoparticles, polymers, biopolymers) that were tested for the foam stability, it still had several shortcomings.¹⁹ It is also noted that each one has its own mechanism to stabilize the foams. In general, the use of high molecular weight additives is not recommended for such studies, since most of them lose their efficiency and have high chances for plugging into the low permeable rock matrix. Among the different additives, the nanoparticle stabilized surfactant foams are witnessed as the most efficient and most commonly studied method. Hence, nanoparticles are considered as one of the best alternatives for the conventional surfactant or polymer stabilized foam due to their extended stability. Nevertheless, the conventional or commercial inorganic nanoparticles fail to stabilize the foams at extreme reservoir conditions due to its surface nature and higher density than organic nanoparticles. In contrast, the modified or functionalized inorganic particles and organic

nanoparticles were found to furnish stable foams even at the harsh reservoir environment by positioning the particles at the gas–liquid interface of the foam and plateau border.^{20–22} Once it gets adsorbed at the interface, the bubbles coalesce or the rupture will be suppressed by reducing the direct contact between gas and liquid. This in turn helps to increase the maximum threshold of the capillary pressure. This further reduces the liquid drainage, coalescence and bubble coarsening, *etc.*^{20,23–25} Despite this the functionalized nanoparticles are more efficient at improving the foam stability, still the use of such costlier and the high concentration (>0.5 wt%) chemicals are considered to be economically non-viable methods for field-scale applications. In most cases the process of surface functionalization is an extremely costly procedure. Hence, it is highly necessary to explore the alternative chemicals that have the capability to stabilize the foam in harsh environments with cheaper technology.

In the past decade, the development of ionic liquids (ILs) has been materialized as the most efficient, and eco-friendly technology candidature for several applications, including oilfield studies. ILs is a kind of organic molten salts, in which the organic cation is fused with either organic or inorganic anions. In general, they are in liquid state at ambient conditions or below 100 °C. Also, they possess excellent physicochemical properties, such as, high solubility, high stability (thermal and chemical), high solvation capacity, negligible vapor pressure, non-flammability, *etc.* Moreover, the physicochemical property of these ILs can be tuned by substituting different types of cations and anions as per the targeted applications.^{26,27} Recently, many researchers have explored the applications of ILs in several fields, such as, separation, de-emulsification, de-asphalting, bitumen extraction, heavy oil upgradation, oil recovery on sandpack, oil–water interfacial tension reduction, wettability alteration, *etc.*^{28–35}

In the recent past, we have synthesized a large number of ILs from various families, such as, imidazolium, alkyl-ammonium, and lactam-based ILs, *etc.*, and studied them for various applications such as, oil–water interfacial study, sludge dissolution, oil recovery on sandpack, wettability alteration, *etc.*^{31–37} It was noticed that the studied ILs had shown a great impact on the reduction of oil–water interfacial tension, wettability modification and thus improved the oil recovery. However, most of these studies were performed at the ambient condition with zero saline or low saline environment. Moreover, in all these cases we have screened only one monovalent ion (NaCl), which does not represent the realistic reservoir condition. Typically, the majority of the oilfield at Saudi Arabian reservoirs are extremely salty with a huge composition of various mono- and divalent ions (TDS = 241 000 ppm).

Some researchers have also studied the solution chemistry of surfactant and ILs binary mixtures, and measured their physicochemical properties. In many cases, it was observed that the surface activity of the surfactant and ILs mixtures were increased more synergistically than their individual fluids.^{38,39} It is one of the essential and pre-requisite properties that are required for the EOR agent in order to boost the oil production.^{31–37} Nonetheless, the interaction between the ILs and



surfactants varies depending on many factors such as, type of charges, hydrophobicity, concentrations, structural orientation of ILs and surfactant molecules, *etc.* In general, the aggregation between ILs and surfactant tend to be instigated by the simple electrostatic interactions of cations and anions (catanionic: cation–anion) from both ILs and surfactants, such aggregates can even alter the surface activity of the combined solution. Many studies have reported that the ILs-surfactant interactions led to the decrease in surface tension and micellar concentration of the mixture than their individual fluids. This is a clear indication that these binary mixtures involve a strong electrostatic interaction between the cations and anions of the ILs and surfactants respectively or *vice versa*. However, it is also varies depending on the ratio of ILs and surfactants.³⁹ Thus, the use of such ILs into the foamability and foam stability is expected to produce a stronger foam with longer stability.

Recently, the author Hanamertani *et al.* (2018)^{19,40} investigated the efficiency of two imidazolium based ILs (1-butyl-3-methylimidazolium bis (trifluoromethylsulfonyl) imide, [C₄mim][NTf₂], and 1-butyl-3-methylimidazolium hexafluorophosphate, [C₄mim][PF₆]), and two choline based ILs, (choline chloride–ethylene glycol [ethaline], and choline chloride–glycerol [glyceline]) for the study of foamability and foam stability at the ambient condition. In this, the author has employed MFOMAX surfactant, (mixture of anionic and amphoteric compositions) with the ILs at the low salinity medium (2 wt% of brine fluid with the composition of NaCl and CaCl₂). Noticeably, the author witnessed a strong indication that ILs have improved the foam stability than the neat surfactant solution. The authors has also demonstrated the conformance control experiments on Brea sandstone sample, and it was noted that the choline ILs has more efficient for the extended foam stability. Though this work is very interesting, in that the author was focused on the sandstone rocks, and studied only one surfactant. Also, the entire study was performed at the low saline medium, unlike the reservoir condition. In reality, the Saudi Arabian reservoirs have a very high salty environment (241 000 ppm of total dissolved salt), with a huge composition of various mono- and divalent ions. Also, it is to be noted that 60% of the world's reservoirs are positively charged oil-wet carbonate rocks, which is completely different from the sandstone rocks (negatively charged water-wet).⁴¹

Though many studies were reported on the use of ILs for numerous applications, only a very limited study was found on foam stability. In fact, no studies were found on the use of ILs for foam stability in the carbonate reservoir at high-temperature, high-pressure, and high salinity. Thus, it is highly essential to investigate the eco-friendly, and inexpensive ILs for the foam studies on the carbonate reservoirs at harsh environments. It is also to be noted that there is still ample scope for screening the various affecting parameters that are influencing the foam stability.

The objective of this study is to assesses the effect of imidazolium based ILs on the carbonate reservoir for the study of foaming and foam stability. Here, we have performed both the bulk and porous scale experiments. In which, we have selected four various ILs with an increase of alkyl-chain length in order to screen the role of hydrophobicity. These ILs are composed of

imidazolium cation and halide (chloride) anion. The colloidal solution of these ILs are highly stable even at harsh temperatures (150 °C) and salinity (240 000 ppm), and also they are freely soluble irrespective of the brine's ionic compositions. Moreover, they are commercially available, eco-efficient, and relatively inexpensive than any other specialized ILs. In the same way, we have selected three various surfactants from three various categories such as, anionic, cationic, and nonionic. These were then studied at the least and effective concentration. At first, we measured the surface tension and particle size (micellar size) of the surfactant solutions with and without ILs. Thereafter, the bulk or static foaming experiments were performed for all those solutions, and evaluated their efficacy on the foamability, and foam stability at the ambient condition. In which we have uncovered various affecting parameters that are involved on the foam stability, such as the types of ILs, ILs concentrations (0–1000 ppm), types of surfactants, types of foaming gases (CO₂, N₂, air), hydrophobicity of ILs, *etc.* Later, the porous or dynamic foaming was performed with the use of coreflood setup. In this, we have studied the best surfactant solution with and without ILs at both atmospheric condition and in high-temperature (80 °C) and correlated their efficacy with static experiments. Subsequently, we also conducted some of the microscopic investigations of the foams with and without ILs in order to understand the mechanism of the ILs on foam stability. Overall, we have witnessed that these ILs are highly efficient for both foamability and foam stability.

2. Experimental section

2.1 Materials: ionic liquids, surfactants, brines, rock sample

For this study, we have employed four different imidazolium based ILs with variation in alkyl chain length, that were purchased from Sigma Aldrich and used as such. They are namely, 1-butyl-3-methylimidazolium chloride [C₄mim]⁺[Cl][−], 1-hexyl-3-methylimidazolium chloride [C₆mim]⁺[Cl][−], 1-octyl-3-methylimidazolium chloride [C₈mim]⁺[Cl][−], and 1-decyl-3-methylimidazolium chloride [C₁₂mim]⁺[Cl][−]. Fig. 1 shows the chemical structures of the ILs with their corresponding abbreviations.

In addition to this, we also studied four various surfactants from different categories, they are namely, alpha-olefin sulfonate (AOS, Al-Biarqi petrochemical Industries Co. Ltd) from anionic, cetyltrimethylammonium bromide (CTAB, Sigma Aldrich) from cationic, fluorosurfactant capstone (FS-31, DuPont Co. Ltd) from nonionic, and 3-(*N,N*-dimethylmyristylammonio) propanesulfonate (betaine; Sigma Aldrich) from zwitterionic category.

In order to emulate the typical Saudi Arabian reservoirs, we have formulated three various brine fluids with variations in salt compositions and used them for this study. They are namely, seawater (SW: TDS = 67 500 ppm), low salinity formation water (LS: TDS = 138 000 ppm) and high salinity formation water (FW: TDS = 241 000 ppm).

Indiana limestone outcrop sample was used for the dynamic foaming experiments. The petrophysical property of the core sample is listed in Table 1.



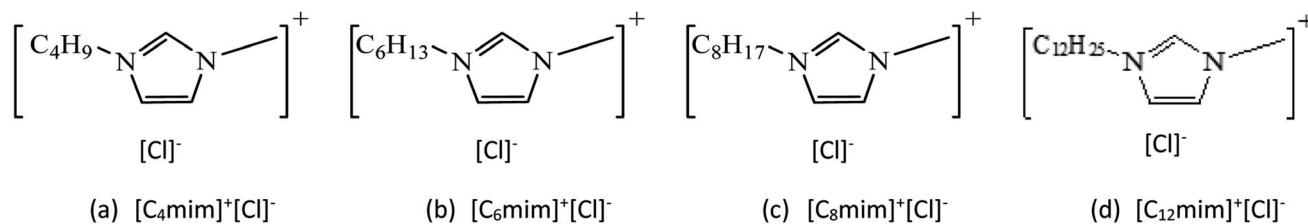


Fig. 1 Chemical structure of the used ILs molecules.

2.2 Characterization of ILs and ILs + surfactant solutions

In this, 0–0.5 wt% or 0–5000 ppm of ILs and 0.02 wt% or 200 ppm of surfactant solutions were prepared and sonicated thoroughly for about 1 h in order to obtain the homogeneous dispersion or solution. Later the binary mixture of ILs + surfactant solutions were formulated for different ILs, and surfactant combinations. Later, they were analysed for the measurement of surface tension and particle sizes with the use of surface tensiometer and dynamic light scattering (DLS) respectively. All these surface tension measurements were performed at the ambient condition using Dynamic Contact Angle Tensiometer (Dataphysics DCAT 11EC, Germany). In this, Wilhelmy platinum–iridium plate (type PT-11; thickness 0.2 mm; area 3.98 mm²; accuracy of $\pm 1.5\%$) was used. In the beginning, the surface tension of seawater was measured to set for a reference case. Later, the ILs, and ILs + surfactant mixtures were screened.

In the same way, particle size or micellar sizes of those ILs and ILs + surfactant solutions were characterized using DLS (Zetasizer Nano series HT, from Malvern) instrument at the ambient condition. In this, we also included the study of salinity contrast to understand the particle or micellar sizes with the increase of salt concentrations. In this, a monochromatic light was exposed on the dispersion fluid and the scattered beam of the light was then passed through the polariser, thereby the particle or the micellar sizes of the dispersion was interpreted. All the prepared solutions were pre-filtered with the use of manual syringe in order to avoid dust particles if any. Also, these measurements were repeated thrice to ensure repeatability.

2.3 Bulk scale foaming

In general, the bulk foam experiments are also called static foaming, where the foaming height (foamability) and foam stability were assessed over time with the use of a time lapse camera. In this, we have screened three foamer gases (CO₂, N₂, and air), three surfactants (anionic, cationic, and nonionic),

and four ILs (50, 100, 200, 500, and 1000 ppm) solutions. Generally, these static foaming experiments are employed as a benchmark to screen the best foamer system with the optimum concentration of ILs and surfactant. Fig. 2 shows the KRUSS dynamic foam analyzer DFA100 (KRUSS GmbH-Germany), which was utilized for all the bulk foaming experiments of surfactant or ILs + surfactant solutions at the ambient condition. This experimental setup consists of a long transparent glass column with a dimension of 250 mm in height and 40 mm in diameter. The bottom of the setup is fixed with a porous filter paper (40–100 μ m). Initially, 50 cm³ or mL of a surfactant or ILs + surfactant solution is used to be filled in the column and then a known volume of gas was injected into the foaming solution to generate the foam. It was injected through the porous filter paper at the bottom of the column. The injection was continued for about 12 s at the flow rate of 0.3 L min⁻¹. Once the foam is formed, all kind of data acquisitions, such as, foam height (foamability), foam half-life (stability), bubble sizes, area of the bubbles, microscopic images of the foams, liquid holdup at the foams interfaces (lamellae) were recorded using the *in situ* installed software of the foam analyzer. In which, the first two parameters of foamability and foam stability are the crucial benchmarks for screening foam efficacy. Foamability is the measurement of foam's height at time zero, and the foam stability is the measurement of the half-life time of the foam over foam decay. Thereafter, the successful system of foaming fluid will be considered for further investigations of dynamic foam generation and transport phenomena at the porous medium using the coreflood apparatus.

2.4 Porous scale foaming

This study evaluates the efficacy of the ILs based foaming fluids for the dynamic foamability at the porous media, which helps to mimic the realistic reservoir condition. In this, we have used a carbonate core (Indiana limestone) sample with the dimensions of 4" length and 1.5" diameter.

Table 1 Chemical composition of the formulated brine fluids

Salt	Seawater (SW) g L ⁻¹	Low salinity formation water (LS) g L ⁻¹	High salinity formation water (FW) g L ⁻¹
NaCl	41.042	75.223	150.446
CaCl ₂ ·2H ₂ O	2.385	34.920	69.841
MgCl ₂ ·6H ₂ O	17.645	10.198	20.396
Na ₂ SO ₄	6.343	0.259	0.518
NaHCO ₃	0.165	0.2435	0.487



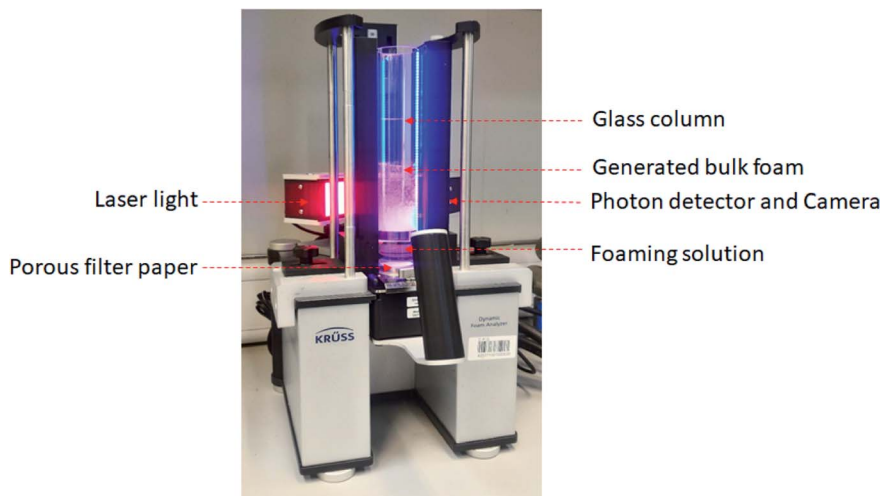


Fig. 2 Experimental set-up used for the bulk foaming analysis.

The petrophysical properties of the core sample, such as pore volume, porosity and permeability were determined and are tabularized in Table 2. Fig. 3a and b shows the pictorial and schematic representation of the coreflood setup used for this dynamic foaming experiment, which consists of a horizontal holder with a 4-inch core sample, accumulators for fluid storages of nitrogen, surfactant and surfactant + ILs solution. The injection of these fluids was facilitated with the use of syringe pumps. The core holder has an in-built electrode at both the inlet and outlet, which is then used to measure the resistance of the system, which was used for the calculation of the water saturation. Initially, the core samples were saturated in their corresponding foaming fluids of surfactant or surfactant + ILs solution under vacuum, and pressurized for 800 psia. Subsequently, the sample was loaded into the core holder. The foams are generated *in situ* through the injection of surfactant alternative gas (SAG) process. In which 0.1 PV of nitrogen (gas) and 0.1 PV surfactant slugs were injected one after another with the constant flow rate of $0.5 \text{ cm}^3 \text{ min}^{-1}$. Both the resistivity and pressure drop across the core were continuously recorded with the use of installed pressure transducers for the entire foam formation and propagation experiment. Later, the measured electrical resistivity was used for calculating the water or gas saturation using Archie's equation as shown below,

$$S_w = \left(\frac{R_0}{R_t} \right)^{1/n} \quad (1)$$

$$S_g = 1 - S_w \quad (2)$$

Table 2 Petrophysical properties of the core samples used for dynamic foam experiments

Rock type	Length (cm)	Diameter (cm)	Porosity%	Permeability (mD)
Indiana limestone	9.96	3.75	18.5	105.2

where, S_w is water saturation, R_0 is the electrical resistivity of the 100% surfactant saturated rock sample, R_t is the electrical resistivity of the rock when it is saturated with surfactant and gas fluids, n is the saturation exponent derived experimentally. Eqn (2) was used to estimate the gas saturation.

All these studies were performed at the temperature of 25 °C and 80 °C, with the high confining pressure of 2200 psia and back-pressure of 1450 psia. In general, the increase of the differential pressure of the porous media is the indication of foam generation and their fluid flow was diminished more significantly by *in situ* foam formation.²¹ Moreover, in this, we have tested only the best candidature of the ILs and surfactant solution based on the previous bulk foam benchmarks. It is also noted that the measurement of ζ -potential of both rock in seawater and ILs in seawater behaved to be the positively charged particles (Table S1†). Hence, it is expected to have no or very minor ILs loss in the carbonate rocks.

2.5 Microscopic studies

In addition to the static and dynamic foams, we also investigated the foam morphology, bubble size, and shapes with the use of microscopes. In this, we have analyzed these parameters with the use of confocal (FV3000, Olympus FluoView) and optical (Leica, DM 2000) microscopes at the atmospheric condition. For this study, we have prepared the solutions of 0.02% FS-31 in SW with and without 0.05% of IL, $[\text{C}_{12}\text{-mim}]^+[\text{Cl}]^-$. Later, these surfactant solutions were shaken briskly for five minutes, and then a drop of the generated foam was placed in the clean glass plate and analyzed for 3D-bulk foam morphology. Thereafter, the same was repeated with covered slip method, in which we place a drop foam on the glass plate, and it was covered with another thin glass slide (sand-witched) to make a 2D-cover slip. Subsequently, it was also processed for microscopic imaging. This gives better foam methodology. All these experiments were performed at 25 °C, and in ambient pressure, and all these scanned images have a resolution of 500 μm .



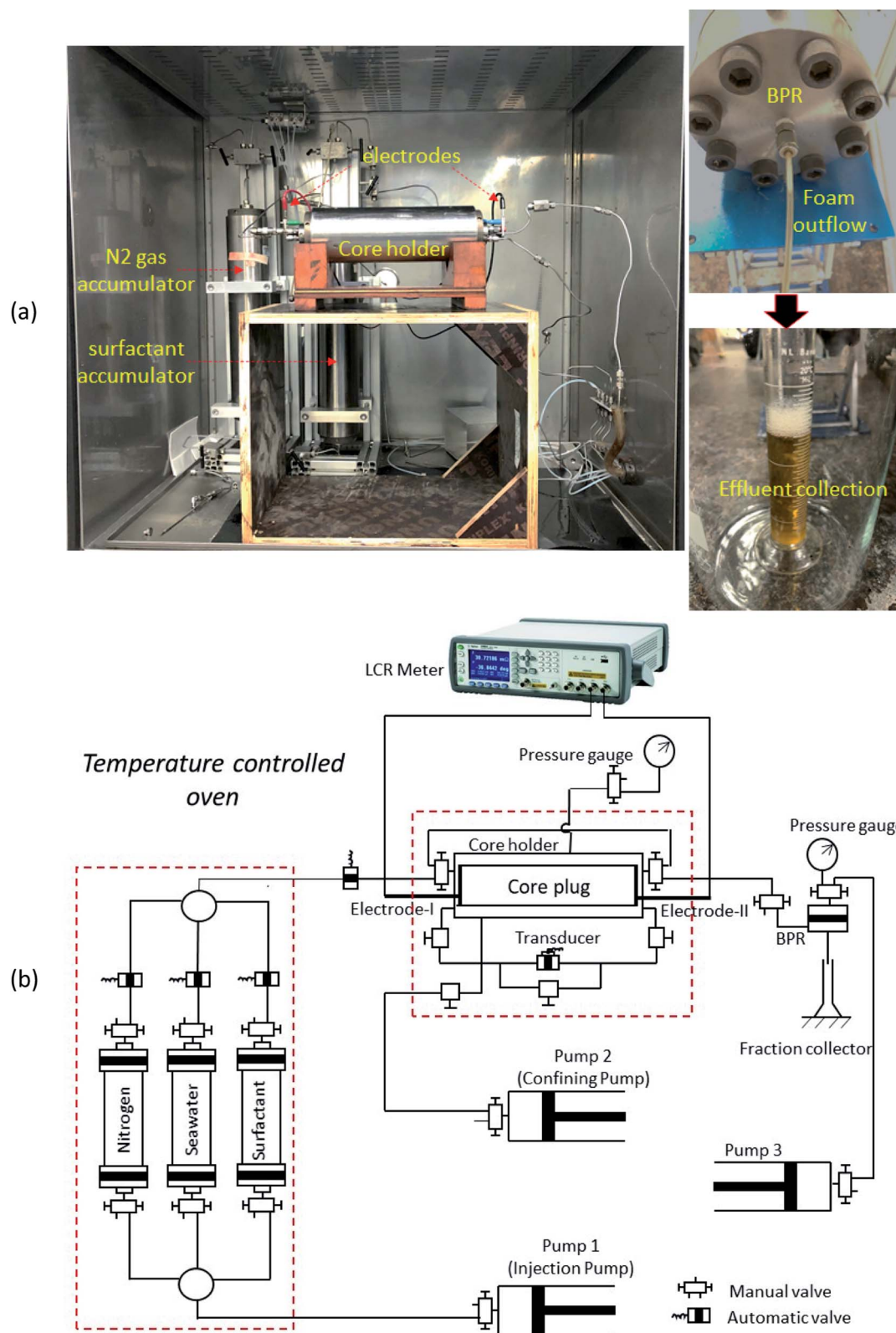


Fig. 3 Pictorial (a), and schematic (b) representation of the coreflood setup used for dynamic foam studies.



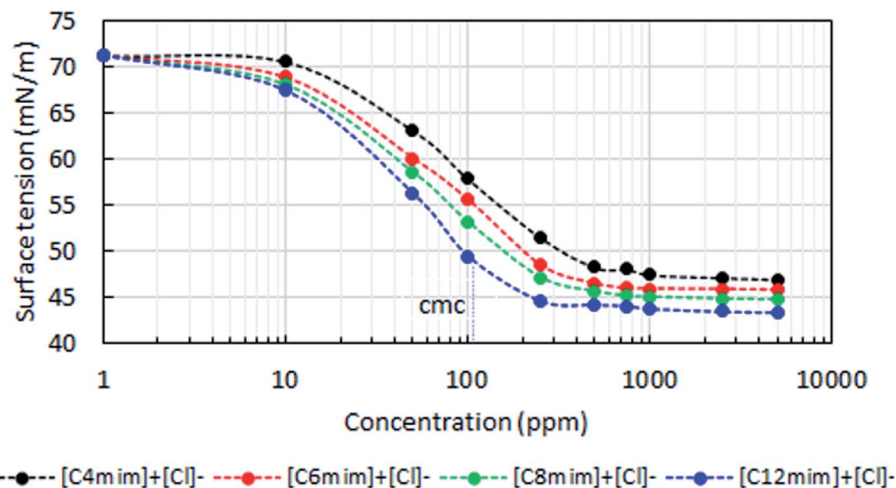


Fig. 4 Surface tension measurements of four different ILs in SW as a function of concentration at atmospheric conditions (25 °C, 14.7 psia).

3. Results and discussion

The first part of this section presents the characterization of various surfactant solutions with and without ILs as a function of type of ILs, type of surfactants, concentrations, salinity, *etc.* Later, the static foamability and foam stability of various surfactant and surfactant + ILs solutions were screened with three different foamer gases. Subsequently, the surfactant and surfactant + ILs solutions were also assessed for dynamic foamability in the carbonate core at high temperature and high salinity. Finally, the possible mechanism for foam stability had also been discussed with the use of some microscopic investigation.

3.1 Surface tension and dynamic light scattering measurements

All the four various ILs solutions were screened for the surface tension measurements in order to obtain the critical micellar concentration (CMC) of each ILs. In this, the measured surface tension data of various ILs were plotted against concentrations. Wherein, the breakpoint of the surface tension curve is

considered to be the CMC of the corresponding system. As seen in Fig. 4, that the addition of ILs reduces the surface tension of the system more abruptly until it reaches the CMC, beyond this no significant changes was observed. This confirms that the addition of ILs tends to adsorb at the air–water interfaces, which reduces the surface tension of the system irrespective of any ILs. However, once it reaches the saturation point or the CMC, the adsorption of ILs on the air–water interface will no longer be entertained, since the interface is already covered with a sufficient amount of ILs layers.⁴²

It is also witnessed that the ILs containing the longer alkyl-chain reduces the surface tension and the CMC to a greater extent than the shorter chain ILs. Similar observations were also witnessed in our previous studies.^{34,43,44} As seen in Fig. 4, that the shorter chain IL, $[C_4mim]^+[Cl]^-$ experiences the CMC at around 255 ppm, whereas in the case of the longer chain containing IL, $[C_{12}mim]^+[Cl]^-$, it was reduced as 110 ppm. We also validated the CMC of these ILs solutions by the measurement of electrical conductivity (Fig. S1†), and the results were in line with the tensiometer findings. This suggest that the high order of hydrophobic interactions (van der Waals force of interactions) would have been experienced between the alkyl-chain

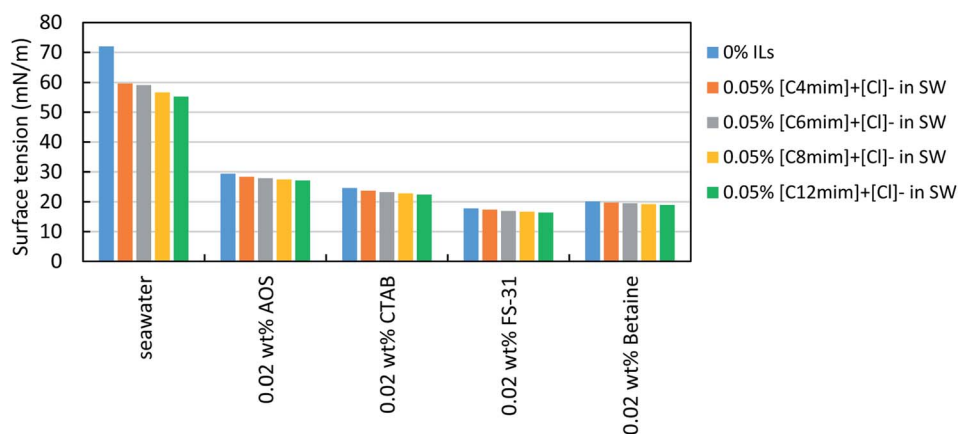


Fig. 5 Surface tension measurements of different surfactant solutions in SW with and without ILs (0.05%) at atmospheric condition (25 °C, 14.7 psia).



moieties of the ILs in the longer chain ILs than the shorter one.⁴⁵ Thus, it enables faster and better aggregations or micellar formation for the longer chain ILs than the shorter ones.

Fig. 5 shows the measurement of the surface tension binary system of surfactant and ILs. Here, three different surfactant solutions (0.02 wt%) were studied with and without 0.05 wt% IL. It was noted that the addition of ILs on surfactant solution further reduced the surface tension of the binary mixture than their individual solutions. Though it is a very marginal effect, it is to be considered as a synergism.⁴³ As a result of this, the surface activity of the surfactant + ILs mixture tends to be increased slightly by exposing more contact area of the liquid phase with the gas phase.⁴⁰ Overall, the lengthier chain ILs works more efficiently on the reduction of surface tension.

Subsequently, the particle or the micellar size distribution of the IL solutions (with and without surfactants) were analyzed using the DLS measurements. In which, the aggregation or micellar size of various colloidal systems were screened as a function of types of ILs, types of surfactants, concentrations, salinity, *etc.* Table 3 shows the measured hydrodynamic diameter of four different IL solution with and without surfactant (0.02%). In this, we have formulated four various concentrations of ILs (50, 100, 500, and 1000 ppm), and studied them with and without surfactant addition (0.02%). As seen in Table 3, it is to be noted that the addition of surfactant on the ILs solution increases the micellar size of the ILs. It is the indication that the ILs and surfactants interact electrostatically, and as a result the micellar sizes of the ILs gets increased by the formation of surfactant layered ILs micellar. However, all these binary solutions (surfactant + ILs) increases the size of the ILs micellar, irrespective of type of surfactant and ILs. Nevertheless, in the case of anionic surfactants, the AOS + ILs mixture has shown

more increment in the micellar sizes than the cationic surfactant of CTAB + ILs. Overall, the order of micellar size increment was found to be noticed as follows; AOS + ILs > FS-31 + ILs > CTAB + ILs.

Similarly, for the case of different ILs, as seen in Fig. 6, it was observed that the longer alkyl-chain length containing ILs have shown an increased micellar size than the shorter chain ILs. Generally, all these imidazolium-based ILs are positively charged in SW solution based on the zeta potential measurement. Wherein, the addition of anionic surfactant with this imidazolium ILs, would certainly increase their micellar sizes by the better electrostatic force of attractions. Whereas, in the case of cationic surfactant it is expected to have a more hydrophobic (van der Waals) force of attractions between the ILs and surfactant, and for the non-ionic surfactant (FS-31), which is expected to experience a combined force of interactions (electrostatic and hydrophobic).

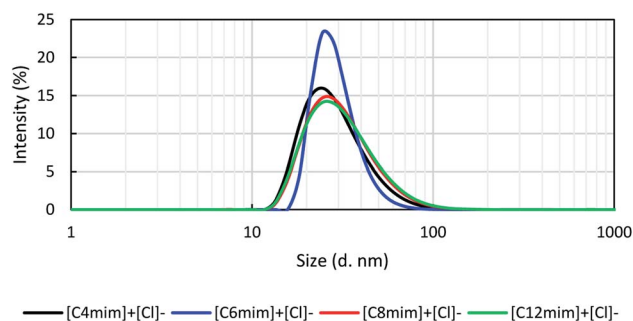


Fig. 6 Hydrodynamic diameter of various ILs (0.05%) in SW at ambient condition (25 °C, 14.7 psia).

Table 3 The hydrodynamic diameter of various ILs (50–500 ppm) in SW with and without surfactants (0.02%) at ambient conditions (25 °C, 14.7 psia)^a

Ionic liquids	Conc. (ppm)	Hydrodynamic diameter (nm)				
		SW (without surf.)	0.02% AOS in SW	0.02% CTAB in SW	0.02% FS-31 in SW	0.02% betaine in SW
[C ₄ mim] ⁺ [Cl] [−]	50	18.5	25.6	22.6	24.3	25.71
	100	20.3	28.9	24.1	27.3	28.78
	500	21.9	36.5	26.3	29.5	32.98
	1000	24.3	37.5	28.0	33.5	33.78
[C ₆ mim] ⁺ [Cl] [−]	50	17.6	33.2	20.1	27.3	27.66
	100	20.9	35.8	20.8	29.3	31.28
	500	22.6	36.7	24.6	32.5	34.88
	1000	25.3	37.5	28.5	35.6	35.76
[C ₈ mim] ⁺ [Cl] [−]	50	21.3	38.6	21.3	30.9	28.32
	100	25.2	39.9	25.3	37.2	32.78
	500	26.3	42.6	27.3	38.2	35.98
	1000	28.3	42.8	28.9	39.7	37.12
[C ₁₂ mim] ⁺ [Cl] [−]	50	22.8	39.1	23.1	32.2	29.91
	100	27.5	42.6	25.6	38.5	34.97
	500	27.9	48.2	28.6	39.9	37.33
	1000	29.6	49.2	30.3	44.1	38.78

^a SW = seawater; the standard uncertainties are $u(T) = 0.1$ K, $u(\text{particle size}) = 2$ nm, $u(\text{conc.}) = 2$ ppm.



Table 4 The hydrodynamic diameter of 500 ppm $[C_{12}mim]^+[Cl]^-$ with and without different surfactants in three brine mediums (SW, LS, FW) at atmospheric condition (25 °C, 14.7 psia)^a

System	Hydrodynamic diameter (nm)		
	SW	LS	FW
Brine conc. (wt%)			
500 ppm $[C_{12}mim]^+[Cl]^-$	27.9	29.1	29.5
500 ppm $[C_{12}mim]^+[Cl]^-$ + 200 ppm AOS	48.2	50.3	52.1
500 ppm $[C_{12}mim]^+[Cl]^-$ + 200 ppm CTAB	28.6	28.9	30.2
500 ppm $[C_{12}mim]^+[Cl]^-$ + 200 ppm FS-31	38.9	39.6	39.8

^a SW = seawater; LS = low salinity; FW = formation water. The standard uncertainties are $u(T) = 0.1$ K, $u(\text{particle size}) = 2$ nm, $u(\text{conc.}) = 2$ ppm.

However, it is also noted that there are no over aggregations that result in any form of precipitation, irrespective of the type of surfactants, ILs, and their concentrations. This confirms that the formulated solutions are highly stable with the combination of any kind of surfactants and ILs. In addition to this, the effect of salinity was also screened on the micellar sizes of the ILs solution, and it is presented in Table 4. A minor increment in the size of micelles was observed with an increase of salinity from seawater to formation water composition. Overall, the change in sizes was in the range of 27.9 to 29.5 nm for different salinities, which indicates that the increase of salinity has no significant impact on neither aggregation nor on the precipitation (sedimentation). A similar response was observed for the case of surfactant + ILs solutions with varying salinity. The observed results have been very promising that the formulated solutions are stable enough even at extreme salinity. Later these formulations were studied for the subsequent studies of foamability and foam stability.

3.2 Bulk-scale foamability and foam stability

Fig. 2 shows the vertical foam analyzer setup that was used for the bulk scale foamability and foam stability experiments. All these experiments were performed at the temperature of 25 °C under atmospheric pressure. All the solutions have been

prepared in SW, and the entire set of studies were performed in three different foamer gas mediums, namely, air, nitrogen and carbon dioxide. In this, we have studied the effect of various parameters, which include the type of ILs, surfactants, foamer gases, hydrophobicity, concentration, and salinity. Table 5 shows the list of all the bulk foam experiments and their corresponding half-life stability.

Initially, the effect of the various surfactant (anionic, cationic, non-ionic and zwitterionic) solutions was screened for the study of foamability and foam stability at the fixed concentration of 0.02%. This study was performed with the intention to set for a reference case to evaluate the new additives, ILs. In this, we have studied all the three different foamer gases of CO₂, N₂, and air. Overall, it was estimated that the air and N₂ based foams were found to be more efficient than the CO₂ gas. This is probably due to the higher solubility of CO₂ gases in brine or the foaming solution. However, as per the concern of different surfactants, the AOS and CTAB have shown better foam stability than the FS-31 in the air gas. Whereas, in the case of N₂ it was noted that the CTAB and FS-31 were more efficient than the AOS.

Subsequently, the effect of ILs concentrations were screened in the range of 50–1000 ppm. Fig. 7 shows the effect of ILs $[C_{12}mim]^+[Cl]^-$ concentrations on the foam stability of FS-31 surfactant (0.02%) solution with different foamer gases (also refer Table 5). It can be noted that with the increase of ILs concentration, the foam stability also increases irrespective of any type of foamer gases. The addition of 50 ppm ILs itself have doubled the half-life time of the foam stability. As observed in Fig. 7, when varying the concentrations of ILs as 50, 100, 200, 500 and 1000 ppm for the system of FS-31 (0.02%) + $[C_{12}mim]^+[Cl]^-$ + air, the half-life stability of the foams had also increased as, 5428, 5589, 5835, 5924, 6012 s from 2155 s. Similarly, for the same system with N₂ and CO₂ gases, the half-life stability increased substantially from 2108 to 4856 s and 265 to 895 s, respectively with the gradual addition of ILs. However, the increase of ILs concentration more than 200 or 500 ppm had no significant improvement on the foam stability, hence it can

Table 5 Half-life time of the various foaming fluids as a function of different ILs, surfactant, concentration, and gas types at ambient conditions

Additives and their half-life time (s)										
Surfactant conc. wt%	Gas type	No. ILs	$[C_{12}mim]^+[Cl]^-$					$[C_8mim]^+[Cl]^-$	$[C_6mim]^+[Cl]^-$	$[C_4mim]^+[Cl]^-$
			50 ppm	100 ppm	200 ppm	500 ppm	1000 ppm	500 ppm	500 ppm	500 ppm
200 ppm AOS	CO ₂	277	709	735	769	845	884	811	778	769
	N ₂	1696	3698	3789	4025	4236	4458	4213	4189	4029
	Air	3054	5219	5436	5689	5896	6012	5816	5742	5682
200 ppm CTAB	CO ₂	247	654	681	695	756	771	743	723	708
	N ₂	2040	3102	3286	3689	3845	4159	3658	3609	3588
	Air	3258	4789	4839	4936	4989	5102	4956	4859	4831
200 ppm FS-31	CO ₂	265	735	761	789	869	895	845	821	810
	N ₂	2108	3915	4251	4586	4725	4856	4518	4326	4259
	Air	2155	5428	5589	5835	5924	6212	5891	5806	5754
200 ppm betaine	CO ₂	251	722	741	775	803	833	791	774	770
	N ₂	891	3788	3855	4077	4311	4612	4278	4244	4188
	Air	2256	5266	5477	5578	5855	5997	5811	5761	5697



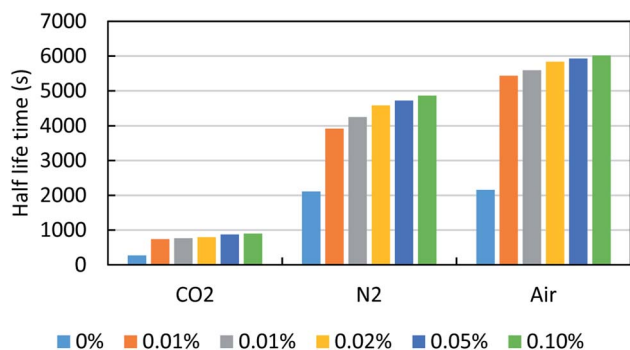


Fig. 7 Effect of ILs, $[C_{12}mim]^+[Cl]^-$ concentrations on the foam stability of FS-31 surfactant (0.02%) solution with different gas foamers.

be ascertained that 500 ppm is the optimum ILs concentration, since it is the lowest concentration with the highest efficiency. After which there is no significant improvement, particularly for air and CO_2 .

Thereafter, the effect of various ILs were screened as a function of hydrophobicity or alkyl-chain length of the ILs. Fig. 8 shows the effect of four various ILs with three different surfactant (0.02%) solutions in three different gas mediums. All these studies were performed at a fixed concentration of ILs, 500 ppm. As seen in Table 5, the increase of alkyl-chain length in the cationic head of ILs increases their ability to boost the foam stability compared to their shorter alkyl-chain ILs. For instance, in the case of lower alkyl-chain ILs, $[C_4mim]^+[Cl]^-$ in AOS solution it had shown the half-life time as 769, 4029, and 5682 s when the medium of gases were CO_2 , N_2 , and air respectively. Later, the same study was performed for the case of lengthier alkyl-chain IL, $[C_{12}mim]^+[Cl]^-$ (500 ppm) also, and here the measured half lifetime was found to have increased significantly as, 845, 4236, and 5896 s at the medium of CO_2 , N_2 , and air correspondingly. Though the differences are minor, it is obvious that higher the hydrophobicity of the ILs better the efficacy in balancing its interaction more appropriately in between air-liquid interface.^{34,43,45} A similar trend of foam stability was observed for all type of surfactants. However, the surfactant of FS-31 had shown relatively better efficiency than

the other two surfactants. Particularly the cationic surfactant, CTAB was found to be least efficient, which may be due to the weaker interaction of CTAB with ILs, since both of them are positively charged, unlike the others.

Subsequently, we also examined the foamability or the foam height for each experiment after generating the foams at time, $t = 0$, and it was plotted on the secondary Y-axis of Fig. 8. Overall, the addition of ILs with any surfactant increases the foaming ability substantially. However, this also depends on other parameters such as gas type, ILs hydrophobicity, surfactant-ILs interactions. As seen in Fig. 8 the maximum foamability was observed in the case of surfactant + ILs with the air medium, and the neat surfactant with the CO_2 gas was identified as the least performer. This could probably be due to the high (dissolution) saturation of CO_2 in water.⁴⁶ Also, the ILs containing longer chains exhibited increased foamability to some extent than the shorter chain ILs of the same family. As discussed in the previous section, the addition of ILs with the surfactant solution reduces their surface tension furthermore synergistically, consequently, which increases the foamability.

Fig. 9 shows the effect of different ILs on the foam decay studies of the 0.02% FS-31 + N_2 system with and without ILs

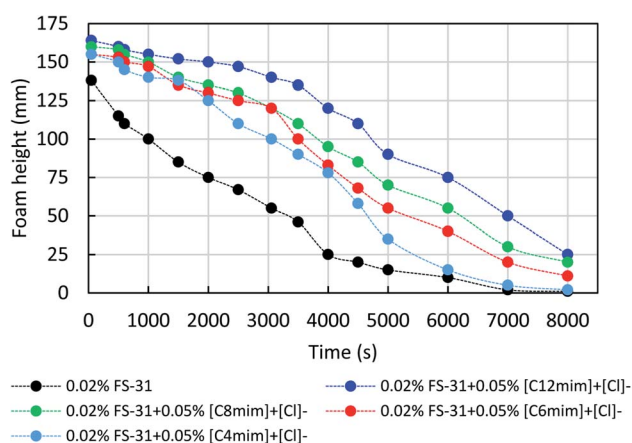


Fig. 9 Effect of four various ILs on the foam decay profile of the 0.02 wt% of FS-31 surfactant solution in N_2 foam at 25 °C.

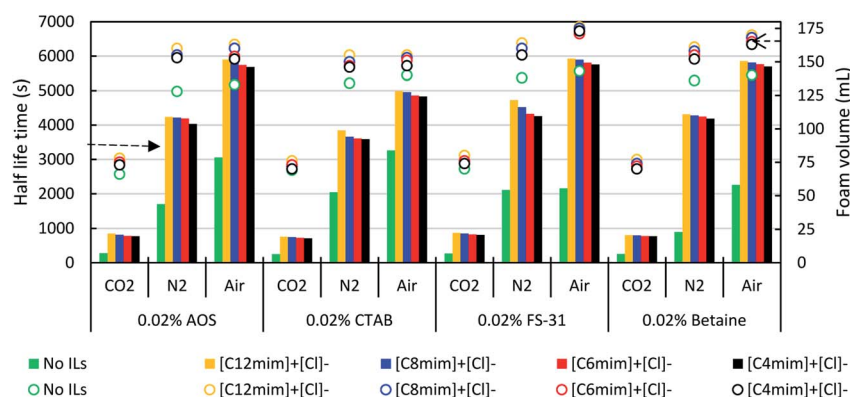


Fig. 8 Foam stability and foamability of three various surfactant solutions with and without ILs (0.05 wt%) in three different foamer gases (CO_2 , N_2 , air). Bar lines correspond to the left side (primary) Y-axis, dotted lines correspond to the right side (secondary) Y-axis.

(500 ppm) at the atmospheric conditions. In this, the ILs added system, 0.02% AOS + 500 ppm IL + N₂, had shown a clear difference, that their foam decay is inhibited and delayed more significantly than the surfactant alone system. Moreover, the longer alkyl chain containing IL, [C₁₂mim]⁺[Cl][−] system works more efficiently for delaying foam decay to a greater extent than the other shorter alkyl-chain ILs. The synergistic stabilization of foams by surfactant + ILs systems mainly depends on the interplay of ILs-interface, surfactant-interface, and ILs-surfactant interactions. In this, the employed imidazolium ILs are typically more of positive charges (based on the zeta potential measurements), and especially the longer alkyl-chain containing ILs are more positively charged than the shorter chain ILs. On the other hand, the surfactant FS-31 is a fluorocarbon surfactant, which is substituted with more electronegative fluorine, along with ethoxy group. Thus, it is expected to enhance the electrostatic force of attraction between the cationic head of ILs with ethoxy part of surfactant moiety. In the same way, it is also expected to experience a hydrophobic force of interactions between the alkyl group of ILs and surfactant (van der Waals force of attractions).⁴⁵ It is further confirmed with the study of surface tension measurements of ILs + surfactant mixtures, as discussed before (3.1.1). As seen in Fig. 5, the surface tension of the ILs + surfactant mixture tends to be reduced synergistically than their individual fluid's surface tension, which confirms that the surface activity of the surfactant solution is boosted upon the addition of ILs in the FS-31 solution. Moreover, the arrangement or positioning of hydrophobic alkyl groups of ILs at the air–water interface would facilitate the greater stability of foams.

Fig. 10 shows the impact of the different gases, namely, air, N₂ and CO₂ on the same system of 0.02% FS-31 + 500 ppm of [C₁₂mim]⁺[Cl][−] + gas. As expected, the air and N₂ are more efficient than CO₂, since it has been witnessed that CO₂ gas has a high solubility in brine fluid than air and N₂. Hence, the trapped CO₂ gas in the foam tends to dissolve in the lamellae liquid, so this results in fast rupture by coalescence and poor

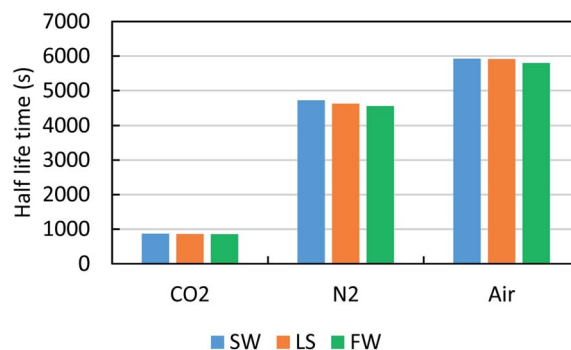


Fig. 11 Effect of salinity contrast on the foam half-life of the 0.02 wt% of FS-31 + 0.05% [C₁₂mim]⁺[Cl][−] solution in three various gas foamers at 25 °C.

stability.⁴⁶ Fig. 11 displays the effect of salinity contrast (SW, LS and FW) on the foam stability of 0.02% FS-31 + ILs system at the atmospheric condition. Usually, the foam stability under extreme saline medium is highly challenging, particularly in the Saudi Arabian reservoirs, wherein the typical salt composition appears to be of such a huge amount (241 000 ppm TDS) with more of di- and monovalent ions. Typically, when increasing the salt concentration, the interactions between the surfactant and additives would get suppressed, which will destabilize the foam stability by precipitation or sedimentation of foaming fluids.^{9,10} In this case, the 500 ppm of [C₁₂mim]⁺[Cl][−] in 0.02 wt% of FS-31 solution was analyzed at different salinity and different gas types. As seen in Fig. 11, it is to be noted that the increase of salinity causes a very mild drop in the foam stability irrespective of any gas type. Overall, these formulated ILs based foams are stable enough with a minor disruption over salinity, thereby overcoming the aforementioned drawback, and portraying their ability to sustain under harsh saline conditions.

Fig. 12 shows the correlation of the number of bubble counts and the mean bubble area of the foams with and without ILs, [C₁₂mim]⁺[Cl][−] on the 0.02 wt% FS-31 surfactant system in the medium of air. It was noted that the addition of ILs on the surfactant solution increased the number of bubble counts very distinctly, at the same time the mean bubble area was reduced drastically. The ILs added system have a greater number of bubble count with lesser mean bubble area which means the system has a large number of smaller bubbles with reduced bubble area over the addition of the ILs on the surfactant solution. As seen before, the addition of ILs reduces the surface tension of the solution, thereby which energizes the production of more bubbles with smaller bubble sizes. In the same way, the liquid drainage of the formulated foams was also investigated with and without ILs on the 0.02% of FS-31 surfactant solution. As expected the addition of ILs controlled the liquid drainage more significantly than the surfactant alone system by adsorbing the ILs at the gas–liquid interface that could resist or slow down the film drainage.⁴⁷ Also, this could increase the maximum threshold capillary pressure through lamellae thickening and increased surface tension.¹¹ Overall, the ILs

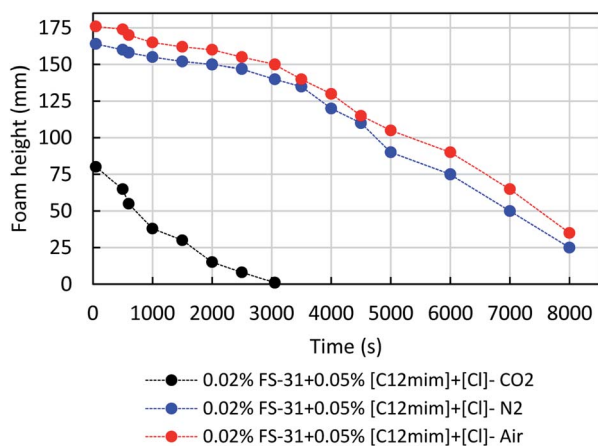


Fig. 10 Effect of three different foamer gases on the foam decay profile of the 0.02 wt% of FS-31 + 0.05% [C₁₂mim]⁺[Cl][−] system at 25 °C.

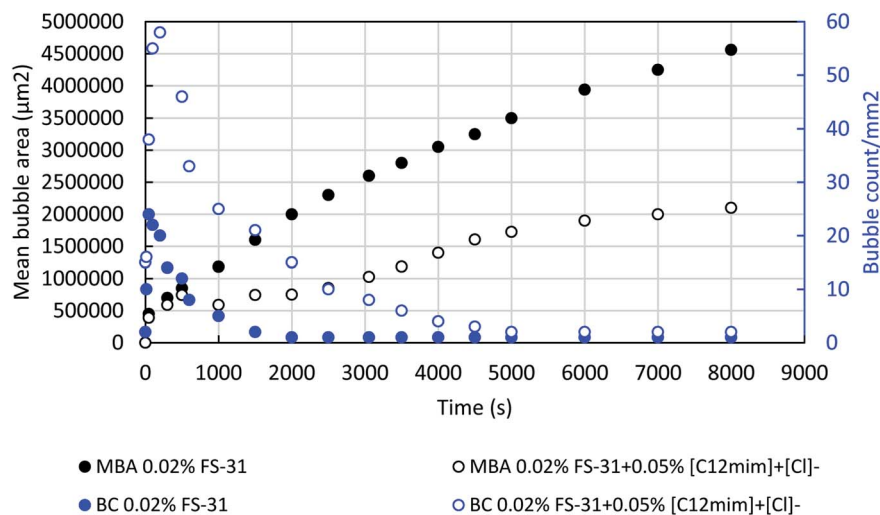


Fig. 12 Effect of IL on the bubble count/mean bubble diameter of the 0.02 wt% FS-31 solution at 25 °C. MBA and BC stand for mean bubble area and bubble count respectively. Filled circles correspond to the mean bubble area; empty circles correspond to bubble counts.

added system is more promising than the surfactant alone system for both the foamability and foam stability.

Fig. 13 shows the microscopic images of the different surfactant solutions with and without ILs at different time intervals (aging time). All these solutions were prepared in seawater medium with N_2 as the foamer gas at ambient conditions. As seen in Fig. 13, the addition of ILs have distinguished the foam sizes more evidently, which was driven by the reduction of surface tension of the system. This can be further backed by examining the bubble sizes of FS-31 with other surfactant solutions. As discussed before, the FS-31 had shown better surfactancy by reducing the surface tension to a greater extent than the other two surfactants, which results in better foamability for FS-31 (smallest bubbles). It was further improved with the addition of ILs, particularly the lengthier alkyl-chain containing ILs, and it is the visible indication that ILs were enhancing the foam stabilization by positioning the ILs molecules at the air–water interfaces (film thickening), which also results in the decrease of film drainage. It is also noted that with the increase of the aging time, foams collapse due to the pressure difference between the bubbles. Young–Laplace effect is the driving force for increasing the bubble size over time which means the pressure differences between two bubbles is the reason for gas diffusion from smaller bubbles to bigger bubbles (Ostwald ripening).⁴⁷

3.3 Porous-scale dynamic foaming experiment by coreflood apparatus

In continuation with the static foams, we also studied the dynamic foamability and their stability to understand the *in situ* foam generation and propagation process in the porous media. In this, we have used the Indiana limestone sample with the dimensions of 4-inch length and 1.5-inch diameter. For this study, we selected only the best surfactant, FS-31 and best IL, $[C_{12}mim]^+[Cl]^-$ based on the benchmark experiments from the bulk foam analysis. First, we have performed the dynamic

foamability of 0.02% FS-31 and 0.02% FS-31 + 0.05% IL, $[C_{12}mim]^+[Cl]^-$ solutions at 25 °C, and in high pressure, 2200 psi. Later, the same was repeated at high temperature, 80 °C and high pressure (2200 psi) to assess the efficacy of ILs on the foam stabilization at the reservoir condition. The constant flow rate of $0.5 \text{ cm}^3 \text{ min}^{-1}$ was maintained for all these studies. All these solutions were prepared in the SW medium, and we have used only N_2 gas for all these studies.

As stated before, we have monitored the measurements of the change of differential pressure and resistivity data throughout the experiments. In this, we have followed the method of the surfactant alternate gas (SAG) injection process for all of our studies. Before beginning the foaming experiments, the core samples were saturated well enough with the foaming fluids to nullify the impact of adsorption of any surfactant or ILs + surfactant fluids on the rock surface during coreflood tests. Fig. 14 shows the pressure drop profile obtained for the solution of 0.02% FS-31 with and without ILs for both 25 °C and 80 °C, at 2200 psi conditions. The observed average pressure drop was recorded as a maximum of 34 psi around 130 min for the neat surfactant solution, 0.02% of FS-31 at 25 °C. For the case of ILs addition, it was increased to 62 psi for the same experimental condition, which means the pressure drop has almost doubled with the addition of ILs. A similar response was observed for the high temperature (80 °C) and high-pressure (2200 psi) experiments as well. In which the neat surfactant resulted only in 25 psi of max pressure drop, and for the ILs added system it went up to a maximum of 51 psi. As expected the increase in temperature causes a slight reduction in pressure drop than their low temperature. It means the foam stability had been suppressed a bit with an increase of temperature by the decreased foam lamellae thickness at high temperature. However, the addition of ILs had increased both the foamability and foam stability than their neat surfactant solution irrespective of temperature, pressure, and salinity.



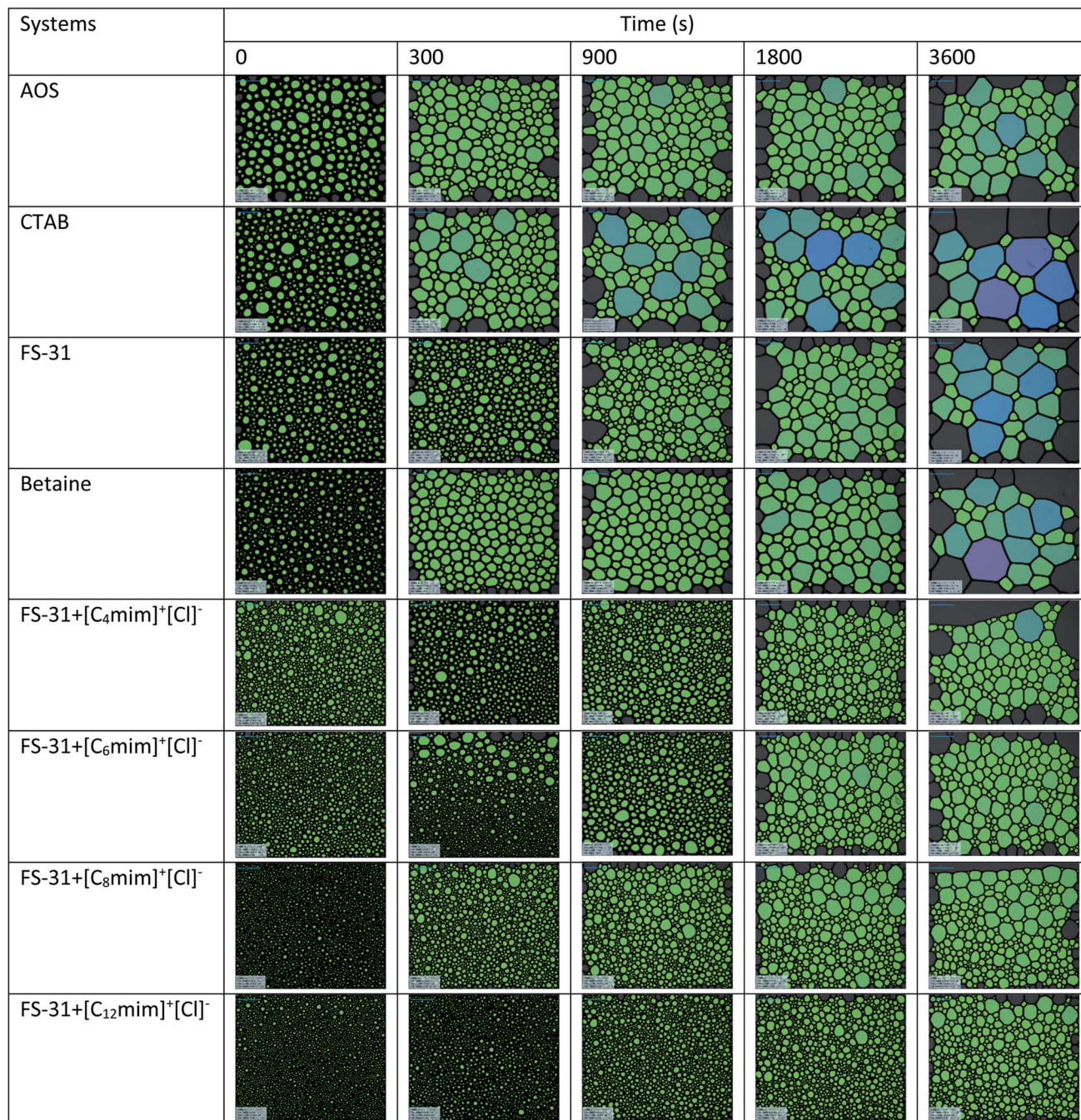


Fig. 13 Microscopic images of the different foaming systems of various surfactant (0.02 wt%) solution with and without ILs (0.05 wt%) at 25 °C.

In addition to this, we also estimated the water saturation profile of the core samples with the use of Archie's equation. Wherein, the measured resistance data was substituted into the Archie's equation to obtain the saturation profile. As stated before, the *in situ* resistivity was measured using the inserted Pt electrodes at both the inlet and outlet. Fig. 15 shows the water saturation profile during the *in situ* foam generation with 0.02% FS-31 solution with and without ILs at both 25 °C and 100 °C. It can be observed that the ILs added surfactant system had shown more reduction in the water saturation than the

surfactant alone system. This conveys that the addition of ILs had increased the foam quality by increasing the gas (N₂) concentration. This is a clear indication that ILs helps to increase the capillary threshold for the foam, thereby this further led to increases the foam stability. Also, the ILs stabilized foam may be experiencing higher apparent viscosity, which will helps to divert the foam flow direction from high permeable zone to the low permeable zone. Furthermore, it is assumed that the foam lamellae will be strengthened with the presence of the ILs, which boosts up the foam stability. Once



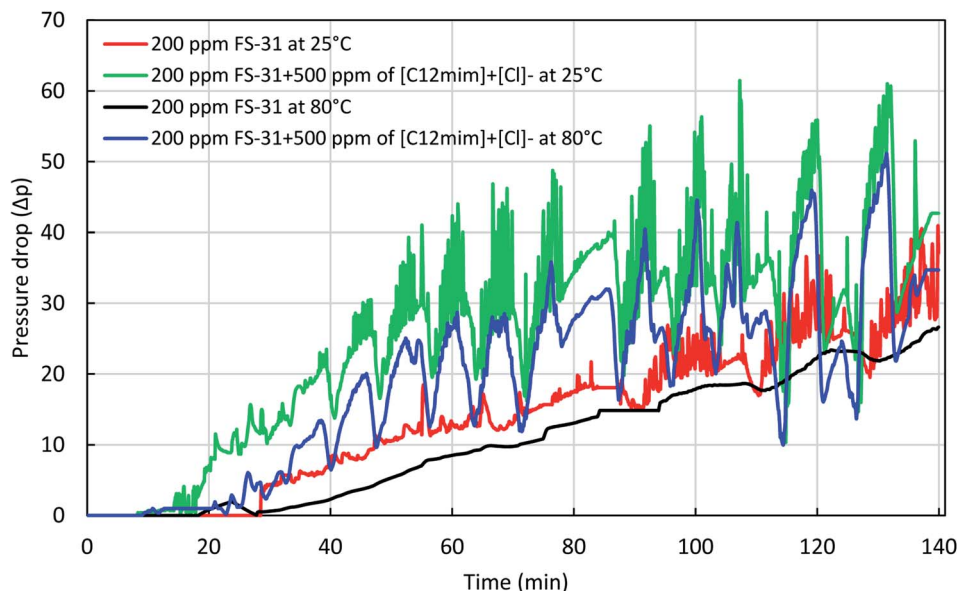


Fig. 14 Pressure drop profile for the injection of 0.02 wt% FS-31 solution on the carbonate sample with and without ILs (0.05 wt%) at the condition of 25 °C and 80 °C, with 2200 psi confining pressure.

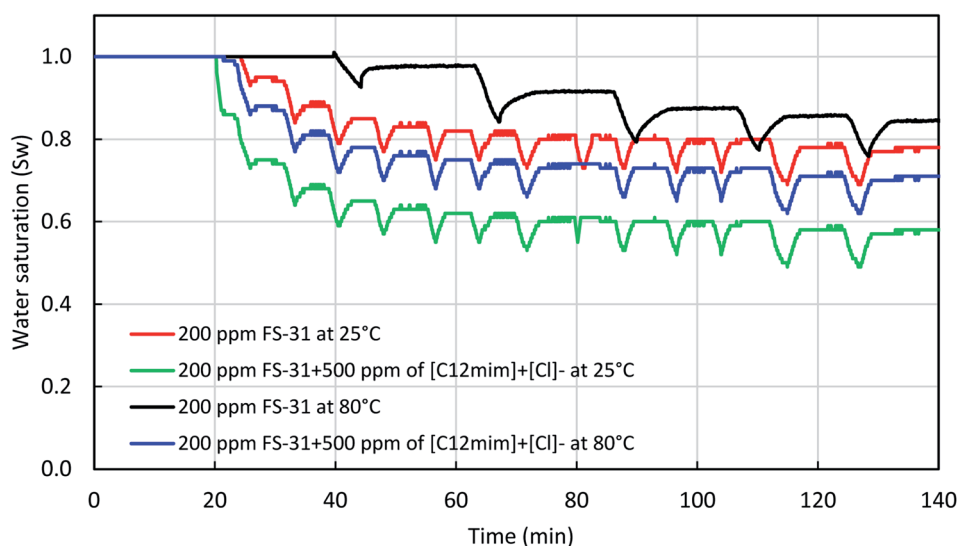


Fig. 15 Water saturation profile for the injection of 0.02 wt% FS-31 solution on the carbonate sample with and without ILs (0.05 wt%) at the condition of 25 °C and 80 °C, with 2200 psi confining pressure.

the foam reaches maximum stability the bubbles get ruptured before regeneration of the bubbles begins. This is how the ILs stabilized foam will assist in enhancing the sweeping efficiency for oil recovery.

3.4 Microscopic studies

In this, we have investigated the air-based surfactant foams with the use of confocal and optical microscopes to attain a detailed stability mechanism. Here, we have analyzed the foam morphology, which includes the structure, size, and shape of the foams of 0.02% FS-31, and 0.02% FS-31 + 0.05% ILs systems at the atmospheric condition. All these foams were studied by

both bulk and covered slip method. Fig. 16 shows the foam morphology of 0.02% FS-31 system in air with and without ILs, where the foaming structure was recorded from 30 s to 1 min after placing the foam on the glass plate. Generally, the observation of this study implies that the addition of the ILs on the surfactant (FS-31) system has helped to increase the lamellae and reduces the irregular shape of the bubbles, making it relatively homogeneous and has reduced the bubble size. Dense lamellae and plateau border is the indication that ILs are positioning more at the air–water interfaces. This is the direct evidence that these ILs have the capability to enhance the foam morphology by accumulating the ILs in the lamellae/plateau



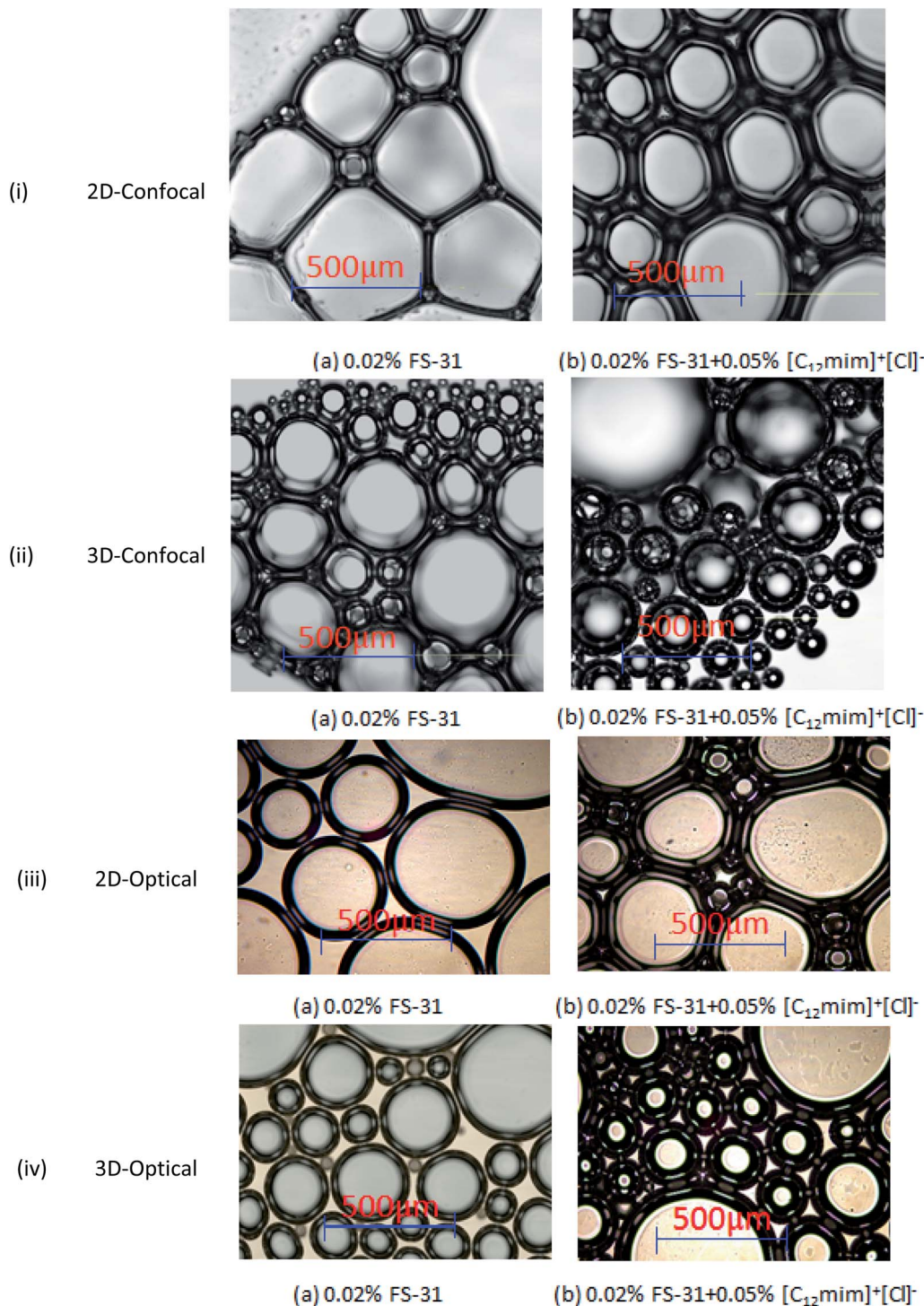


Fig. 16 Confocal and optical microscopic images of the 0.02% FS-31 foam film in air medium with and without ILs (0.05 wt%) by both covered slip (2D) and bulk foam (3D) methods.

border, by which their film thinning and bubble coalescence have been suppressed more considerably.^{9,48}

Moreover, in the ILs added system, it has been observed that the bubbles are more spherical in shape and smaller in size than the surfactant alone system, which could be due to the increased interfacial elasticity (viscoelasticity) of the foams by adsorbing the ILs at the gas–liquid interface¹¹ leading to

increase in foam stability. The interfacial elasticity of the foams is a crucial factor that determines the foam stability in the reservoir condition, particularly in the foam transport phenomenon. Hence, the foams which are formulated with the addition of ILs have shown better stability in the porous media as shown in the previous section of dynamic foam stability. Overall, the added ILs helps to retard the bubble coalescence or



coarsening by thickening the lamellae film and holding the pressure back in the smaller bubbles. Moreover, these bubbles are tight enough than the surfactant alone system. However, it is also necessary to study the effect of oil-tolerance for the ILs stabilized foams to obtain the complete evaluation, which is in-planning to further clarify and quantify this contribution.

4. Conclusion

Systematically, four different ILs solutions were characterized for their colloidal stability with and without surfactants using tensiometer and DLS measurements. It was noted that the formulated ILs solutions are extremely stable irrespective of any salinity and temperatures. Thereafter, the static foaming experiments were performed with the addition of these ILs on various surfactant solutions at three various foamers of air, N₂ and CO₂. In this, the ILs added systems had improved foamability and foam stability of any surfactant solutions. Moreover, the foams were observed to be highly stable in air and N₂ than CO₂, since CO₂ had been highly saturated in the foaming solution, unlike air and N₂. In the case of different ILs, it was witnessed that the ILs which had longer alkyl-chain exhibited higher stability and high foamability than the lower or the shorter alkyl-chain ILs.

Simultaneously, the dynamic foam stability of the surfactant solutions with and without ILs were evaluated using the typical coreflood experiments at high temperature, high pressure and high salinity. Based on the measured differential pressure and water saturation of various systems, it was witnessed that the addition of ILs to surfactant solution shows a significant improvement of the foam stability in the porous media than the neat surfactant solution. In addition to this, the measured surface tension of the foaming surfactant solutions were decreased synergistically with the addition of ILs on the surfactant solution. In addition, the microscopic investigations of the foams revealed that the addition of the ILs causes them to arrange in the gas-liquid interface of the foam bubbles and aids to increase the lamellae size. Mechanistically, it is suggested that the positioning of ILs on the gas-liquid interface of the foam bubbles is the key phenomenon to thickening the lamellae. Further, it leads to increase in the maximum with-standing capillary pressure of the bubbles and suppresses the bubbles coalescence/film thinning/liquid drainage/rupture. This study confirms that these employed ILs are highly potential for the study conformance control even at the high-temperature, high-pressure, and high-salinity, thus it can also be considered as the best alternative for the conventionally used EOR agents.

Conflicts of interest

There are no conflicts to declare.

Acknowledgements

The authors would like to acknowledge CIPR, CPG, KFUPM for the lab facility.

References

- 1 S. Velusamy, S. Sakthivel and J. S. Sangwai, *Energy Fuels*, 2017, **31**(8), 8764–8775.
- 2 Z. AlYousef, M. Almobarky and D. Schechter, *Energy Fuels*, 2017, **31**, 10620–10627.
- 3 M. M. Almajid and A. R. Kavscek, *Adv. Colloid Interface Sci.*, 2016, **233**, 65–82.
- 4 W. R. Rossen, C. J. van Duijn, Q. P. Nguyen, C. Shen and A. K. Vikingstad, *SPE J.*, 2010, **15**, 76–90.
- 5 A. H. Falls, G. J. Hirasaki, T. W. Patzek, D. A. Gauglitz, D. D. Miller and T. Ratulowski, *SPE Reservoir Eng.*, 1988, **3**, 884–892.
- 6 Q. Sun, Z. Li, S. Li, L. Jiang, J. Wang and P. Wang, *Energy Fuels*, 2014, **28**, 2384–2394.
- 7 T. Blaker, M. G. Aarra, A. Skauge, L. Rasmussen, H. K. Celius, H. A. Martinsen and F. Vassenden, *SPE Reservoir Eval. Eng.*, 2002, **5**, 317–323.
- 8 A. R. Kavscek and H. J. Bertin, in: *SPE/DOE Improved Oil Recovery Symposium*, Society of Petroleum Engineers, 2002.
- 9 N. Yekeen, M. A. Manan, A. K. Idris, A. M. Samin and A. R. Risal, *J. Pet. Sci. Eng.*, 2017, **159**, 115–134.
- 10 T. Zhu, D. O. Ogbe and S. Khataniar, *Ind. Eng. Chem. Res.*, 2004, **43**(15), 4413–4421.
- 11 N. Yekeen, M. A. Manan, A. K. Idris, E. Padmanabhan, R. Junin, A. M. Samin, A. O. Gbadamosi and I. Oguamah, *J. Pet. Sci. Eng.*, 2018, **164**, 43–74.
- 12 T. J. Myers and C. J. Radke, *Ind. Eng. Chem. Res.*, 2000, **39**, 2725–2741.
- 13 L. L. Schramm, in: *Foams: Fundamentals and Applications in the Petroleum Industry*, 1994, pp. 165–197.
- 14 M. Simjoo, T. Rezaei, A. Andrianov and P. L. J. Zitha, *Colloids Surf., A*, 2013, **438**, 148–158.
- 15 R. Farajzadeh, A. Andrianov, R. Krastev, G. J. Hirasaki and W. R. Rossen, *Adv. Colloid Interface Sci.*, 2012, **183–184**, 1–13.
- 16 R. M. Sunmonu and M. Onyekonwu, in: *Society of Petroleum Engineers – 37th Nigeria Annual Int. Conf. and Exhibition, NAICE 2013 – To Grow Africa's Oil and Gas Production: Required Policy, Funding, Technol., Techniques and Capabilities*, Society of Petroleum Engineers, 2013, vol. 2, pp. 1061–1073.
- 17 S. Babamahmoudi and S. Riahi, *J. Mol. Liq.*, 2018, **264**, 499–509.
- 18 S. I. Kam and W. R. Rossen, *SPE J.*, 2003, **8**, 417–425.
- 19 A. S. Hanamertani, R. M. Pilus, N. A. Manan and M. I. A. Mutalib, *J. Pet. Sci. Eng.*, 2018, **167**, 192–201.
- 20 A. Maestro, E. Rio, W. Drenckhan, D. Langevin and A. Salonen, *Soft Matter*, 2014, **10**, 6975–6983.
- 21 M. Khajepour, S. R. Etminan, J. Goldman, F. Wassmuth and S. Bryant, *SPE J.*, 2018, **23**, 2232–2242.
- 22 R. Singh and K. K. Mohanty, *Energy Fuels*, 2015, **29**, 467–479.
- 23 S. I. Karakashev, O. Ozdemir, M. A. Hampton and A. V. Nguyen, *Colloids Surf., A*, 2011, **382**, 132–138.
- 24 S. Li, Z. Li and P. Wang, *Ind. Eng. Chem. Res.*, 2016, **55**, 1243–1253.



- 25 J. Yu, C. An, D. Mo, N. Liu and R. L. Lee, in. *SPE Improved Oil Recovery Symposium*, Society of Petroleum Engineers, 2012.
- 26 N. V. Plechkova and K. R. Seddon, *Chem. Soc. Rev.*, 2008, **37**, 123–150.
- 27 T. Welton, *Chem. Rev.*, 1999, **99**(8), 2071–2084.
- 28 C. G. Hogshead, E. Manias, P. Williams, A. Lupinsky and P. Painter, *Energy Fuels*, 2011, **25**, 293–299.
- 29 P. Painter, P. Williams and A. Lupinsky, *Energy Fuels*, 2010, **24**, 5081–5088.
- 30 P. Williams, A. Lupinsky and P. Painter, *Energy Fuels*, 2010, **24**, 2172–2173.
- 31 S. Velusamy, S. Sakthivel and J. S. Sangwai, *Energy Fuels*, 2017, **31**, 8764–8775.
- 32 S. Velusamy, S. Sakthivel and J. S. Sangwai, *Ind. Eng. Chem. Res.*, 2017, **56**, 13521–13534.
- 33 S. Sakthivel, S. Velusamy, R. L. Gardas and J. S. Sangwai, *RSC Adv.*, 2014, **4**, 31007–31018.
- 34 S. Sakthivel, S. Velusamy, R. L. Gardas and J. S. Sangwai, *Ind. Eng. Chem. Res.*, 2015, **54**, 968–978.
- 35 S. Sakthivel, S. Velusamy, V. C. Nair, T. Sharma and J. S. Sangwai, *Fuel*, 2017, **191**, 239–250.
- 36 S. Sakthivel, S. Velusamy, R. L. Gardas and J. S. Sangwai, *Energy Fuels*, 2014, **28**, 6151–6162.
- 37 S. Sakthivel and S. Velusamy, *Fuel*, 2020, **276**, 118027.
- 38 G. Y. Wang, Y. Y. Wang and X. H. Wang, *J. Mol. Liq.*, 2017, **232**, 55–61.
- 39 F. Comelles, I. Ribosa, J. J. Gonzalez and M. T. Garcia, *Colloids Surf., A*, 2015, **484**, 136–143.
- 40 A. S. Hanamertani, N. A. Manan, S. Ahmed and R. M. Pilus, in. *Society of Petroleum Engineers – SPE Kingdom of Saudi Arabia Annual Technical Symposium and Exhibition 2018, SATS 2018*, Society of Petroleum Engineers, 2018.
- 41 M. Kanj, S. Sakthivel and E. Giannelis, *Colloids Surf., A*, 2020, **598**, 124819.
- 42 P. Pillai, A. Kumar and A. Mandal, *J. Ind. Eng. Chem.*, 2018, **63**, 262–274.
- 43 S. Sakthivel, P. K. Chhotaray, S. Velusamy, R. L. Gardas and J. S. Sangwai, *Fluid Phase Equilib.*, 2015, **398**, 80–97.
- 44 S. Sakthivel, S. Velusamy, R. L. Gardas and J. S. Sangwai, *Colloids Surf., A*, 2015, **468**, 62–75.
- 45 B. Smit, A. G. Schlijper, L. A. M. Rupert and N. M. Van Os, *J. Phys. Chem.*, 1990, **94**, 6933–6935.
- 46 R. Farajzadeh, A. Andrianov, H. Bruining and P. L. J. Zitha, *Ind. Eng. Chem. Res.*, 2009, **48**, 4542–4552.
- 47 Q. Sun, Z. Li, J. Wang, S. Li, B. Li, L. Jiang, H. Wang, Q. Lü, C. Zhang and W. Liu, *Colloids Surf., A*, 2015, **471**, 54–64.
- 48 Q. Lv, Z. Li, B. Li, S. Li and Q. Sun, *Ind. Eng. Chem. Res.*, 2015, **54**, 9468–9477.

